Design and characterization of a research electrohydraulic lithotripter patterned after the Dornier HM3

Robin O. Cleveland
Department of Aerospace and Mechanical Engineering, Boston University, Boston, Massachusetts 02215

Michael R. Bailey
Applied Physics Laboratory, University of Washington, Seattle, Washington 98105

Naomi Fineberg
Division of Biostatistics, Indiana University School of Medicine, Indianapolis, Indiana 46202

Bruce Hartenbaum
H-Tech Laboratories, Santa Monica, California 90406

Murtuza Lokhandwalla
Graduate Aeronautics Laboratory, California Institute of Technology, Pasadena, California 91125

James A. McAteer
Department of Anatomy and Cell Biology, Indiana University School of Medicine, Indianapolis, Indiana 46202

Bradford Sturtevant
Graduate Aeronautics Laboratory, California Institute of Technology, Pasadena, California 91125

(Received 23 November 1999; accepted for publication 15 February 2000)

An electrohydraulic lithotripter has been designed that mimics the behavior of the Dornier HM3 extracorporeal shock wave lithotripter. The key mechanical and electrical properties of a clinical HM3 were measured and a design implemented to replicate these parameters. Three research lithotripters have been constructed on this design and are being used in a multi-institutional, multidisciplinary research program to determine the physical mechanisms of stone fragmentation and tissue damage in shock wave lithotripsy. The acoustic fields of the three research lithotripters and of two clinical Dornier HM3 lithotripters were measured with a PVDF membrane hydrophone. The peak positive pressure, peak negative pressure, pulse duration, and shock rise time of the focal waveforms were compared. Peak positive pressures varied from 25 MPa at a voltage setting of 12 kV to 40 MPa at 24 kV. The magnitude of the peak negative pressure varied from -7 to -12 MPa over the same voltage range. The spatial variations of the peak positive pressure and peak negative pressure were also compared. The focal region, as defined by the full width half maximum of the peak positive pressure, was 60 mm long in the axial direction and 10 mm wide in the lateral direction. The performance of the research lithotripters was found to be consistent at clinical firing rates (up to 3 Hz). The results indicated that pressure fields in the research lithotripters are equivalent to those generated by a clinical HM3 lithotripter. © *2000 American Institute of Physics.* [S0034-6748(00)01806-2]

I. INTRODUCTION

Shock wave lithotripsy (SWL) is the procedure used in clinical urology by which focused, high energy shock waves generated outside of the body are used to destroy kidney stones. The technique was introduced in 1980[1] and has become so successful that at present more than 85% of renal calculi in the United States are treated by SWL.[2] Despite the widespread popularity of the technique, there is growing evidence that SWL can result in kidney damage.[3,4] The significance of the tissue damage is still under debate, as are the mechanisms which produce it.[5,6] In addition there is no agreement as to the mechanism by which the shock waves comminute calculi.[7]

The groups involved in this manuscript are part of a multi-institutional research program to address issues in SWL. Our interests lie in investigating mechanisms of stone comminution, mechanisms of tissue damage, and the significance of tissue damage. The Dornier HM3 was the first lithotripter introduced into clinical service in the United States and in 1996 was still the most widely used device in the United States.[2] The popularity of the Dornier HM3 led us to focus our experimental efforts on this machine. Our groups work closely with clinical urologists and experiments carried out on an HM3-type device are going to have direct clinical relevance to the largest possible number of cases. There were a number of reasons to fabricate separate research lithotripters for our laboratories rather than rely on clinical machines. First, it is hard to obtain easy access to clinical lithotripters, including retired units. Second, even if access to clinical devices were possible, they are manufactured in a way which necessarily provides few adjustable pa-

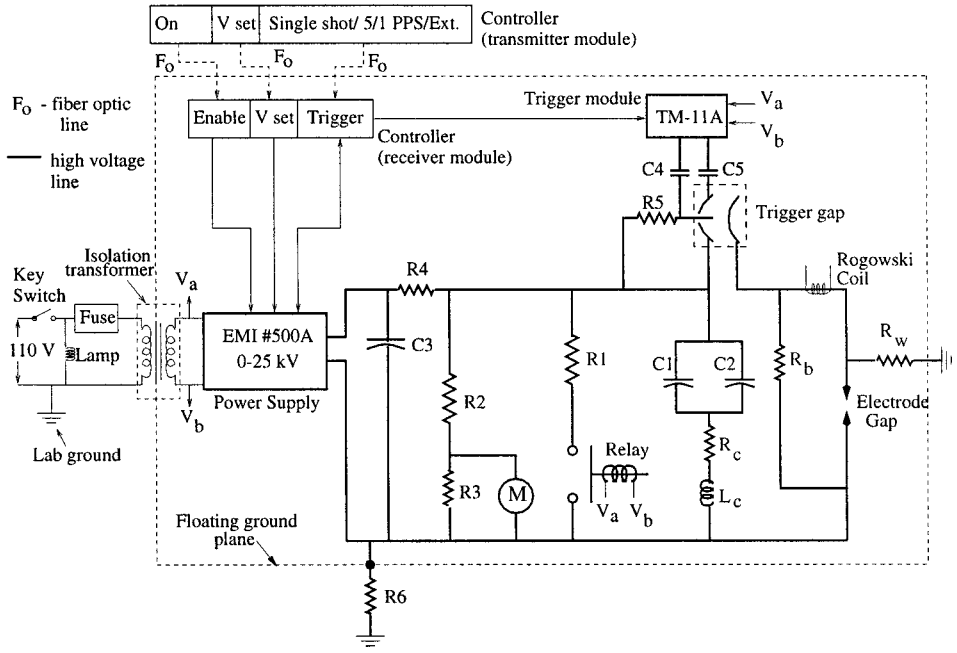

FIG. 1. High-voltage supply and control circuit. Heavy lines designate high-voltage conductors, and light lines are either control lines or are at building supply voltage (110 V).

rameters and so severely restrict the scope of experiments that can be carried out. Finally, the groups are geographically separated and have differing experimental configurations, which makes sharing of a single device impractical. The approach taken was to construct three lithotripters, individually tailored to the needs of each research group, that would provide performance equivalent to the HM3.

The HM3 is an electrohydraulic lithotripter (EHL), that is, it generates a shock wave by creating an electrical breakdown (spark) underwater. A vapor bubble, produced by the spark, grows rapidly and generates a spherically spreading shock wave. The spark is located at the first focus (F1) of a hemiellipsoidal reflector; the shock wave is reflected from the ellipsoid and focuses at the second focal point (F2) of the ellipsoid. Measurements of the acoustic field generated by the Dornier HM3 have been reported in the literature[8–10] and the HM3 has also been included in comparative studies with other clinical lithotripters.[11,12] Other researchers have fabricated research electrohydraulic lithotripters.[13–15] In each of these devices, there are key mechanical and electrical parameters that are not equivalent to the HM3.

The design described here was based on measurements of the characteristics of a clinical HM3. The prototype research machine was constructed at The California Institute of Technology (Caltech) and has been described briefly elsewhere.[16] Three replicate instruments that incorporate modifications to the prototype were subsequently installed at the Applied Physics Laboratory of the University of Washington, Seattle (APL-UW), the Department of Anatomy and Cell Biology, Indiana University School of Medicine, Indianapolis (Anat-IU), and the Graduate Aeronautical Laboratory, California Institute of Technology, Pasadena (GALCIT). In this work, we compared the performance of these three research lithotripters to two Dornier HM3 clinical lithotripters located at Methodist Hospital, Indianapolis.

II. EXPERIMENTAL APPARATUS

A. Research lithotripters

The research lithotripters described here were designed by one of us (B.H.) and constructed at the Graduate Aeronautical Laboratories, California Institute of Technology. We refer to them collectively as the ''Caltech-EHL.'' The design objective was to replicate the mechanical and electrical characteristics that determine the performance of the unmodified Dornier HM3 lithotripter (Dornier Medical Systems, Kennesaw, GA). We note that the term ''unmodified HM3'' refers to the original machine which has an 80 nF capacitance. Dornier later produced a ''modified HM3'' which had a reduced shock wave amplitude, achieved by reducing the capacitance to 40 nF. In addition, the ellipsoidal reflector of the modified HM3 was given a slightly larger aperture to produce a tighter focal zone. The mechanical parameters of the unmodified HM3 that were matched in our design included: the geometry of the ellipsoidal reflector, the angle of the acoustical axis, and the conditioning of the water. Electrical parameters included: the storage capacitance, the voltage on the capacitance, the electrode, and the impedance of the discharge circuitry. Other considerations driving the design were the pulse repetition rate, accuracy of positioning specimens for testing, and the simplicity and safety of operation. The apparatus consists of the following subsystems: (1) high voltage system and control circuit, (2) hemiellipsoidal reflector and test tank, (3) water degassing and storage system, and (4) auxiliary systems.

1. High-voltage supply and control circuit

The essential elements of this subsystem are: a power supply, a pair of capacitors, a triggering unit, and an electrode. A schematic of the circuit is shown in Fig. 1, in which heavy lines designate high-voltage conductors and light lines are either control lines or are at building supply voltage (110 V). The electrical elements of the circuit are listed in Table I.

TABLE I. Electrical specifications of the high-voltage supply and control circuit.

Item	Value	Vendor
Resistor R1	4×0.2 MΩ, 10 kV, 1500 J	Cesiwid Inc, Niagara Falls, NY
Resistor R2	361.4 MΩ, 30 kV, 15 W + 3.92 MΩ, 4 kV, 2 W	Caddock Electronics Inc, Riverside, CA
Resistor R3	36.5 kΩ (4×146 kΩ in parallel)	
Resistor R4	2500 Ω, 45 kV	Cesiwid Inc, Niagara Falls, NY
Resistor R5	1 MΩ	
Resistor R6	1 GΩ, 32 kV, 10 W	Cesiwid Inc, Niagara Falls, NY
Resistor R_b	7.7 kΩ (28×275 Ω)	
Capacitor C1, C2	40 nF, 100 kV, *S* type	Maxwell Laboratories, San Diego, CA
Capacitor C3	0.001 mF, 25 kV dc	Newark, Santa Fe Springs, CA
Capacitor C4, C5	500 pF, 30 kV dc	Newark, Santa Fe Springs, CA
High-voltage cables	AWM 40 kV dc STYLE 3239 VW-1	Rowe, Toledo, OH
Power supply	EMI # 500A, 0–25 kV, POS	Lambda EMI, Neptune, NJ
Trigger module	Model TM-11A	EG&G Electro-Optics, Salem, MA
Triggered spark gap	Model GP-12B	EG&G Electro-Optics, Salem, MA
Isolation transformer	IT25-5E 115 V, 25 kV	Hipotronics Inc, Brewster, NY
Fiber-optics controller	Custom designed	KVA Engineering, Hollister, CA
Electrode	Refurbished Model SG-80 (HM3 & HM4)	Servicetrends Inc, Marietta, GA
Relay	E-40-NC, 40 kV single pole, normally closed, 115 VAC coil	Ross Engineering, Campbell, CA
Grounding Rod	30 kV, 25 J, with 10 feet cable	Ross Engineering, Campbell, CA

The high-voltage power supply is capable of generating voltages in the range 0–25 kV and has an average charging rate of 500 W. The total capacitance of the power pack, C1 and C2, is 80 nF. When discharged from full voltage the capacitors can deliver up to $0.5CV^2=25$ J per pulse; thus the power supply can support a maximum firing rate of 20 Hz. However, other system components limit the maximum pulse rate to 5 Hz. The voltage on the capacitors is monitored by a 10 000:1 voltage divider (R2, R3) and a digital voltmeter M. A normally closed electromagnetic relay short circuits the terminals of the storage capacitors C1, C2. This relay is activated by a key switch. Hence, in case of an accidental power failure, or when the key switch is turned off, the storage capacitors discharge through R1 in about 0.1 s. The power supply is isolated from building power by an isolation transformer. A safety feature of this design is that all the high-voltage circuitry is physically built on a floating ground plane (indicated by a dotted rectangle in Fig. 1), which can be electrically isolated from laboratory ground.

The storage capacitors feed current to a triggered spark gap. The triggered spark gap acts as a rapid switch, which is closed by a trigger module. The triggered spark gap consists of a pair of primary electrodes and a third trigger electrode sealed within a housing. The trigger module applies a high-voltage pulse (15–30 kV, rise time <2 μs, recycle time $\sim$100 ms) between the trigger electrode and one of the primary electrodes; the pulse ionizes the gas to produce a conduction path between the primary electrodes which, in turn, carries the full discharge current from the storage capacitor. Capacitors C4 and C5 provide dc isolation, preventing a discharge from the power pack to the trigger module. The bleed resistor R_b provides a bleed path for the current before the gap break-down, and results in a ''softer'' discharge. The resistor R_c and inductance L_c represent parasitic effects in the circuit. The resistor R_w represents the resistance of the water bath. The Rogowski coil[17] indicated in Figs. 1 and 2 is a current transformer which measures the discharge current and provides a trigger for other equipment, e.g., an oscilloscope. The Rogowski coil is not used in the UW and IU machines, which instead use a photodiode to detect the flash from the underwater spark discharge and trigger other equipment.

The power-pack assembly is shown in Fig. 2. The capacitors and triggered spark gap are enclosed in an acrylic housing. The assembly above the housing converts from the planar geometry of the capacitor system to the coaxial configuration of the Dornier electrode. The hybrid planar/coaxial arrangement of the Caltech EHL differs from the Dornier HM3 which is cylindrical throughout, including eight cylindrical capacitors (10 nF each) held between two circular discs (a fact we discovered after the fabrication of the research lithotripters). The arrangement of the capacitors in the Caltech lithotripters matched the capacitance of the HM3 and had an inductance that was just slightly larger (probably induced by the planar/coaxial transition). The triggered spark gap feeds current through the copper positive feed plate to the center conductor of the coaxial holder. The brass center conductor (positive) of the coaxial holder is 14.5 mm in diameter and 35 mm long. The outer conductor (negative) has a 24 mm inner diameter and 32 mm outer diameter. The two conductors of the coaxial holder are insulated by a machined cylinder with walls 9.4 mm thick made either of phenolic (GALCIT) or Teflon-PTFE (APL-UW, Anat-IU). The end of the coaxial holder was machined to accept the electrode, and electrical connections are made with spring-leaf contacts. Standard Dornier-type electrodes (SG-80) are used. The feedplate and coaxial holder are the principal mechanical support for the spark plug. The end of the coaxial holder is fitted with an aluminum collar so that it can be bolted to the ellipsoidal reflector. An O-ring (Parker 2-020) ensures a water tight seal. The electrode is mated to the ellipsoid by sliding the powerpack into position on a horizontal shelf.

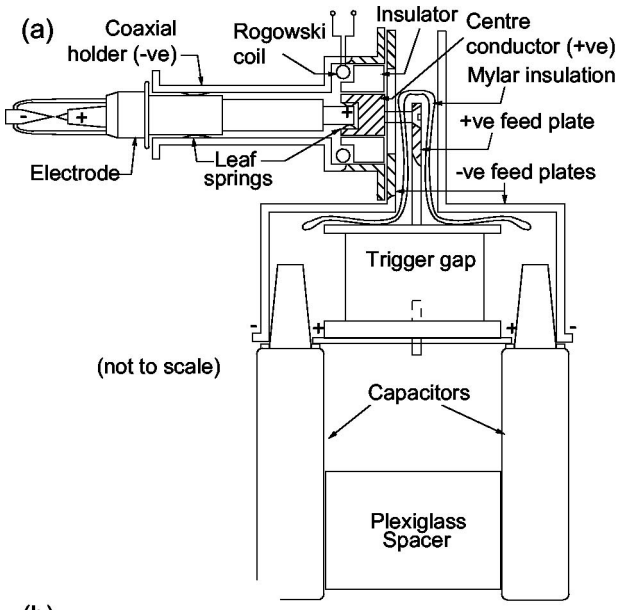

FIG. 2. Power pack assembly: (a) schematic (not to scale) and (b) photograph of a fully assembled power pack (scale is in inches; 1 in.=25.4 mm).

The research lithotripter system is controlled by a pair of modules (transmitter and receiver). The control features include: switching the high voltage on and off, setting the voltage level, and triggering (firing) the lithotripter. The receiver module is housed inside the lithotripter frame and is connected to the transmitter module by fiber optic cables to reduce the risk of danger of electrical shock to the operator. The transmitter can be used to fire the lithotripter manually

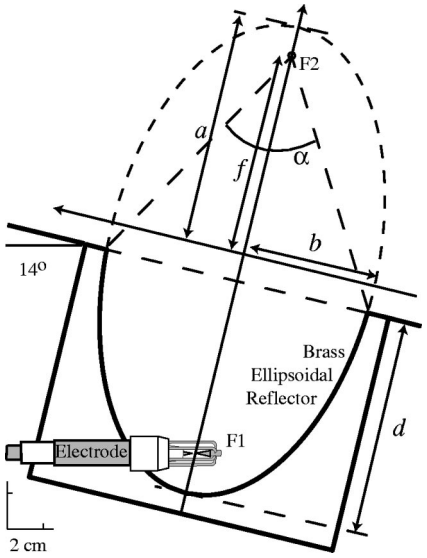

FIG. 3. Ellipsoidal reflector geometry: $a=139$ mm, $b=78$ mm, $d=124$ mm and $f=114$ mm.

or in a pulse mode (1 or 5 Hz). It also has an external trigger so that the lithotripter can be fired by another device, e.g., a computer or function generator.

2. Hemiellipsoidal reflector and test tank

The ellipsoidal reflector (Fig. 3) has same dimensions as that of the unmodified Dornier HM3 lithotripter: semi-major axis $a=139$ mm, semiminor axis $b=78$ mm ($b/a=0.56$, eccentricity $\epsilon=\sqrt{1-(b/a)^2}=0.8$), and the reflector is truncated by 15 mm, that is, it is not a complete hemiellipsoid. The aperture angle of the reflector is $\alpha=68°$ and the direct distance between the two foci is $2f=2\epsilon a=228$ mm. The electrode is located at the internal focus (F1) of the hemiellipsoid and is oriented at 76° to the major axis. The 14° inclination of the ellipsoid's major axis results in F2 being horizontally offset from F1, ensuring that bubbles generated near F1 do not interfere with specimens at F2. The ellipsoid is bolted to the bottom of the water tank and sealed with RTV silicone gel. The Caltech EHLs are supplied with a fixed position stylus, similar to that provided with the HM3, to locate the geometrical focus of the ellipsoid. In addition, the APL-UW lithotripter is fitted with two small laser pointers attached to either the side of the test tank and aligned with the focus of the lithotripter.

Three different test tanks were made to the specifications of each research group. They are all rectangular, and of such a size that the path lengths of transmitted or scattered waves from F2 to the free surface or a wall are all approximately equal and sufficiently large that return waves do not intrude on measurements at F2 during experimental times of interest. The GALCIT test tank was made of welded aluminum plate 13 mm thick. It has a footprint of 610×610 mm and its height varies from 460 to 610 mm due to the inclination of the bottom of the tank. Opposite side walls are fitted with 150 mm diameter optical quality windows centered at F2. The test tank at APL-UW was constructed of clear acrylic to provide complete visual access. The walls are 13 mm thick and the footprint of the tank is 580×950 mm; height varies

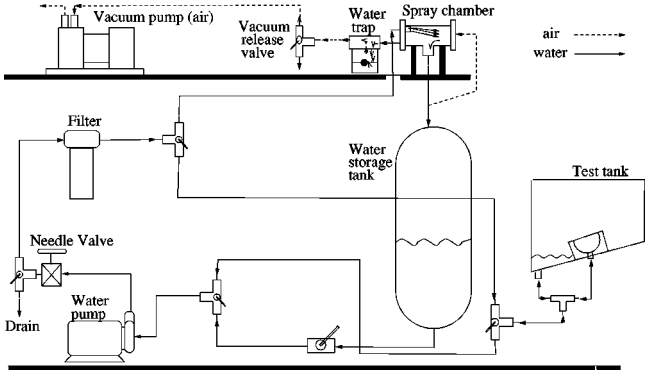

FIG. 4. Water degassing and storage system.

from 360 to 590 mm. The test tank at Anat-IU was made from a 610×610×610 mm polyethylene tank with walls 8 mm thick (Model 6324, U.S. Plastics).

3. Water degassing and storage system

It was necessary to design a water processing system for the research lithotripters for vacuum degassing, filtering, and storing water. The motivation for degassing and filtering the water is to reduce cavitation along the shock wave axis, as excessive numbers of bubbles can interfere with propagation of shock waves. Figure 4 shows a schematic of the system; the essential components are listed in Table II.

When the system is in degassing mode, water is pumped from the storage tank (0.25 m^3 capacity), passed through the filter (0.5 μm) and into the spray chamber. The spray chamber is evacuated to an absolute pressure of about 20 kPa (0.8 atm vacuum) by the vacuum pump. The water is sprayed into the chamber through a nozzle with 20 holes each of 1 mm diameter; the spray increases the surface area of the water and accelerates the degassing process. The system can reduce the O_2 content of the water in the storage tank to below 5 ppm within 1 h. The water can be stored under vacuum to maintain low levels of dissolved gas. Transfer of the degassed water to the lithotripter tank is done at atmospheric pressure through the centrifugal pump. While sitting in the test tank the water regasses at a rate of about 1 ppm/day. The pump takes about 10 minutes to fill the test tank, and delivers 12 ℓ per minute against a head of 135 kPa. The water is softened by adding either NaCl or $NaHCO_3$ until a conductivity of 660 μS/cm is achieved. The degassing and softening of the water is very similar to the Dornier HM3 water processing system. For *in vitro* experiments which require temperature control, the specimen is surrounded by an enclosure and the water heated with an immersion heater.

4. Auxiliary systems

The research lithotripters were equipped with motor driven *X-Y-Z* positioners that could be controlled by handheld joystick or computer (Velmex-Unislide, East Bloomfield, NY). It proved necessary to insert optical isolators between the mechanical limit switches for the slides and the motor controller because transients from the spark discharge would appear on the limit switch wiring and damage the controller.

B. Clinical lithotripters

Measurements were conducted on two clinical unmodified Dornier HM3 lithotripters located at Methodist Hospital, Indianapolis. They are referred to as HM3-A and HM3-B. The *X-Y-Z* gantry and fluoroscopic localization systems used to position patients for treatment were used to position the hydrophone for waveform determinations. Templates of the shock wave axis were fitted to each of the fluoroscope monitors and were used to orient the sensitive element of the membrane hydrophone to predetermined points of a mapping grid. A small radiopaque marker was placed on the sensitive spot of the hydrophone and was removed before shock wave measurements were taken.

C. Instrumentation

All pressure measurements reported here were carried out with a commercial polyvinylidene fluoride (PVDF) membrane hydrophone (model 301, Sonic Industries, Hatsboro, PA) designed explicitly for lithotripsy measurements. The manufacturer specifies that the response of the PVDF membrane is flat up to 50 MHz. The membrane has a nominal active diameter of 0.5 mm and is provided in a cartridge format so that a PVDF membrane can be easily replaced once it has been damaged. A control unit monitors the resistance of the electrodes on the membrane and informs the user when too much erosion has occurred. The hydrophone is unshielded and must be operated in deionized water (less than 5 μS/cm) making it incompatible with the weak electrolyte which fills the lithotripter tank. Therefore, an isolation tank (22×32×30 cm) was constructed so that the hydrophone could be immersed in deionized water. The deionized water in the small isolation tank was degassed using a multiple pinhole degassing system.[18] The bottom of the isolation tank was fitted with a thin sheet (100 μm) of low density polyethylene (LDPE). The effect of the sheet (ascertained by comparing the effect of two sheets to one sheet) was negligible. One would anticipate that the LDPE would slightly attenuate the waveform and increase the rise time of

TABLE II. Description of components in water processing subsystem.

Item	Part number	Vendor
Centrifugal water pump	8249K62	McMaster-Carr, Atlanta, GA
Diaphragm vacuum pump	DAA-V174-EB	Gaast, Benton Harbor, MI
Filter housing	P-01509-00	Cole-Parmer, Vernon Hills, IL
5 μm filter cartridge	P-01509-15	Cole-Parmer, Vernon Hills, IL
Spray chamber: 4 in.×4 in. Tee	72-4487	Westchem Equipment Inc. Livermore, CA
Water trap (8 oz)	AA672K	Brenner-Fiedler, Cerritos, CA

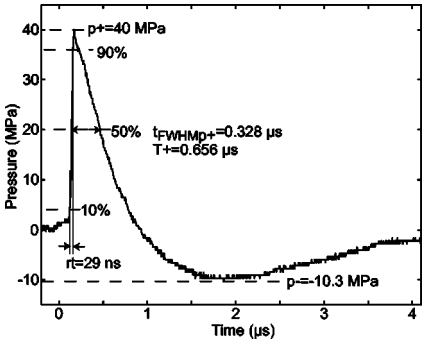

FIG. 5. Shock wave parameters: peak positive pressure $p+$, peak negative pressure $p-$, duration of the positive phase T_+, and rise time rt.

the shock wave. However, the effect of the LDPE sheet on the rise time was smaller than the minimum resolvable rise time of the PVDF membrane hydrophone; the effect of the LDPE on the amplitude was also not resolvable.[19]

Waveforms were recorded on a digital storage oscilloscope (Tektronix, Beaverton, OR), transferred to computer using Labview (National Instruments, Austin, TX), and saved to disk for later analysis. Post processing was done with Matlab (Mathworks, Natick, MA). The data were converted to pressure using the calibration value provided with the membrane cartridge. For approximately half of the cartridges we verified the calibration values over the range of 2–20 MHz by substitution calibration[20] with a Marconi PVDF membrane hydrophone (type Y-33-7611, Marconi, UK) that had been calibrated at the National Physical Laboratory (NPL, Teddington, UK). The calibrations provided with the cartridges were found to be accurate to within 10% which is similar to the uncertainty in the NPL calibration.

The parameters that were obtained from each waveform are shown in Fig. 5. The peak positive pressure $p+$ and peak negative pressure $p-$ were determined directly from the maximum and minimum pressure in the waveform. Note that for measurements off-axis, it was important to choose an appropriate time window, as the edge of the membrane generated a scattered wave artifact that could be larger than the acoustic waveform.[21] The duration of the positive phase T_+ was assumed to be twice the duration of the full width half maximum (FWHM) $t_{\mathrm{FWHM}p+}$ which is defined[22] as the interval between the time when the acoustic pressure first exceeds 50% of $p+$ to the next time that the pressure has that value. The duration of the negative phase was not calculated as measurements of lithotripsy shock waves using a fiber-optic hydrophone indicate that PVDF membrane hydrophones may artificially shorten the duration of the negative phase of the waveform.[23] Other parameters, including the peak negative pressure $p-$, were not significantly different between the fiber-optic and PVDF membrane hydrophones. The rise time was the time taken for the pressure to increase from 10% to 90% of $p+$. We note that rise time measurements were limited by the hydrophone. The 50 MHz bandwidth is commensurate with a resolvable rise time of approximately 20 ns, where as the theoretical steady-state rise time of 40 MPa step shock is 0.15 ns.[24]

Electrohydraulic lithotripters display significant shot-to-shot variation because of jitter in the location of the arc discharge. It is therefore necessary to record a number of shots at each condition to determine the statistics. However, because the shock waves damage the hydrophone it was necessary to limit the number of shots fired at each condition. We recorded at least ten shock waves for each measuring condition, a number that has been used previously.[12] After each shock wave the LDPE sheet and the PVDF membrane were cleared of visible bubbles using a pipette. Bubbles can interfere with the measurement of a shock wave and can seed cavitation that damages the membrane. Shock waves were fired at approximately 5 s intervals, except for the pulse rate tests. For all measurements, electrodes were ''preconditioned'' with 50 shock waves (at 18 kV) and were not used for measurements beyond 2000 shock waves. The majority of the data presented here were for electrodes with less than 1000 shots.

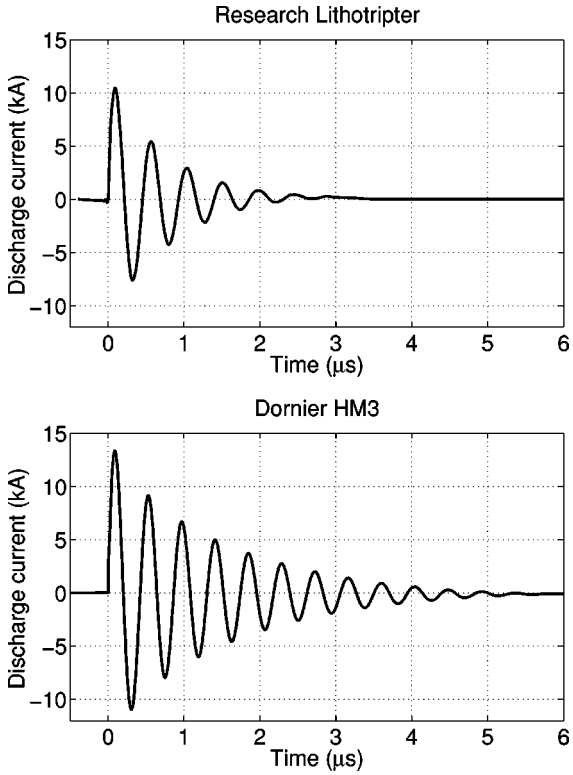

FIG. 6. Discharge current measured by the Rogowski coil. $V_0 = 18$ kV, shorted electrode. Top, GALCIT EHL; bottom, HM3-A.

III. RESULTS

A. High-voltage system

The characteristics of the high-voltage system were measured during a spark discharge. Figure 6 shows the current measured by the Rogowski coil during the discharge of shorted electrodes in both the GALCIT lithotripter and the HM3-A clinical machine. The maximum current of the HM3-A is about 30% larger than that of the GALCIT EHL. Given a capacitance of 80 nF, measurements of the frequency and decay time of these traces can be used to calculate the circuit inductance L_c and the resistance R_c. These are given as a function of capacitor discharge voltage for both the GALCIT EHL and the HM3-A in Fig. 7. The GAL-

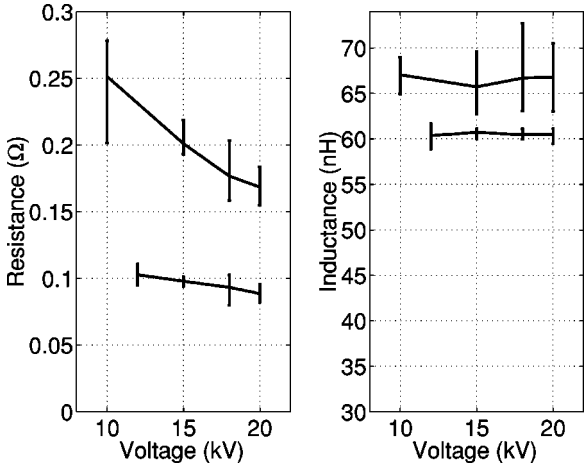

FIG. 7. Resistance R_c (left) and inductance L_c (right) of the lithotripter spark supply circuits. Top curves, GALCIT EHL; bottom curves, HM3-A. Note the truncated scale of inductance.

CIT machine showed more scatter than the HM3-A, and the resistance of the GALCIT machine varied more strongly with the supply voltage. Both of these features are attributable to differences between the EG&G trigger switch and the switch used in the Dornier HM3. The higher resistance in the research lithotripters is probably associated with parasitic resistance in both the trigger gap and the capacitors. Quantitative results for L_c and R_c at 18 kV, and values from other research machines, are given in Table III. The effect of the larger inductance of the research lithotripters is to slightly reduce the resonant frequency of the circuit, from 2.28 to 2.17 MHz, and that of the increased resistance is to reduce the number of cycles during which the discharge current decays, from 11 to 5. Since the rise time of the current pulse is nearly the same in the two machines, the parameters of the shock waves generated by the Caltech EHLs are expected to reproduce those of the HM3. The major consequence of the substantially larger resistance in the Caltech lithotripters should be that the capacitor life is extended. When the spark is struck in water, as during the normal lithotripter operation, the plasma gap adds an additional variable resistance to give a total resistance (for the GALCIT EHL) of $0.233 \pm 0.013\ \Omega$, while other measured parameters remain the same. In comparison to reported values for other research lithotripters, we observe that the Caltech machines very closely mimic the parameters of the HM3.

B. Acoustic field

The acoustic fields of all five lithotripters were measured. Figure 8 shows representative waveforms measured at the geometrical focus in each of the lithotripters with a setting of 18 kV. The slight jitter in arrival time is associated with uncertainty in triggering and does not indicate a systematic difference between the lithotripters. The mean value and standard deviation, based on 10 successive shock waves, for the parameters defined above are given in Table IV. It can be

TABLE III. Inductance and resistance at 18 kV.

Machine	L_c (nH)	R_c (Ω)
HM3-A	60.5±0.4	0.093±0.008
GALCIT EHL	66.7±2.8	0.177±0.012
Coleman *et al.*	250	0.3
Prieto *et al.*	300	0.86

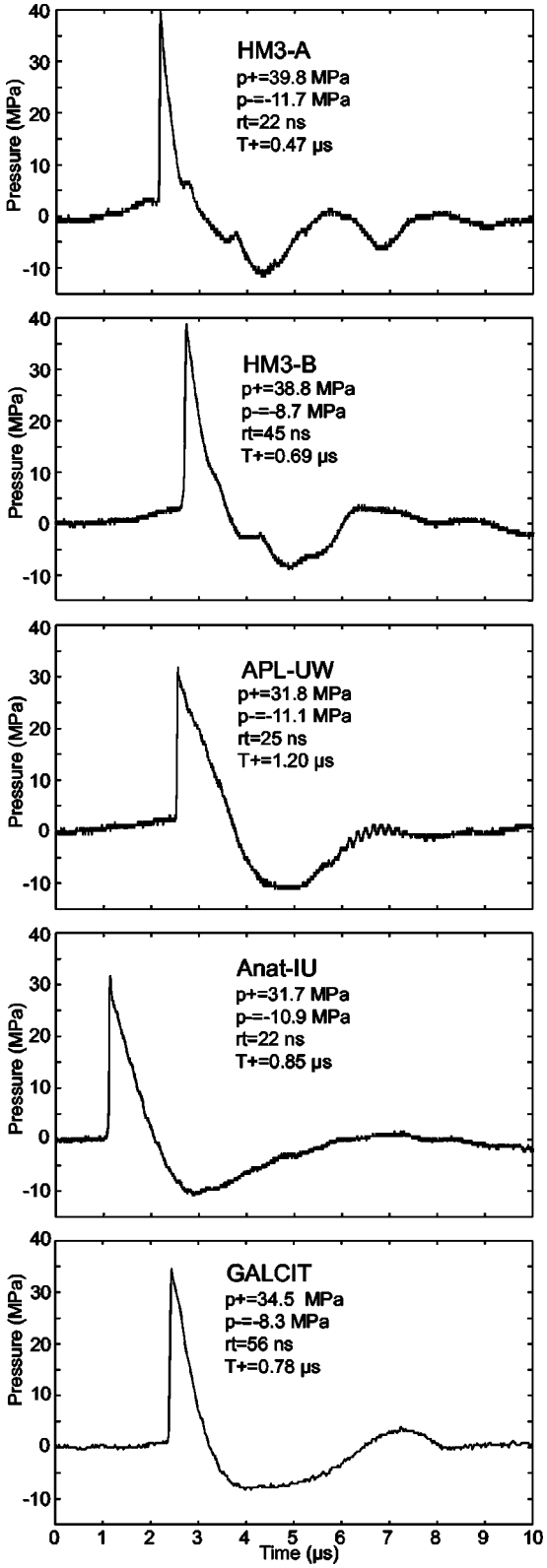

FIG. 8. Representative waveforms measured in the different lithotripters at the geometrical focus with a discharge voltage of 18 kV.

TABLE IV. Comparison of pulse parameters for the two HM3 lithotripters and the three research lithotripters at 18 kV.

Quantity	HM3-A	HM3-B	APL-UW	Anat-IU	GALCIT
$p+$ (MPa)	38.4±6.2	34.0±5.3	29.9±4.7	30.3±10.2	35.3±5.4
$p-$ (MPa)	10.0±1.4	8.7±0.8	11.5±0.3	11.1±0.9	8.7±0.4
rt (ns)	49±14	59±12	28±8	26±8	50±4
T_+ (μs)	0.62±0.17	0.92±0.16	1.2±0.2	1.0±0.3	0.82±0.15

seen that the peak positive pressure measured was about 38 MPa in HM3-A, 35 MPa in GALCIT, 34 MPa in HM3-B, and 30 MPa in APL-UW and Anat-IU. The peak negative pressures were all around −10 MPa. The negative pressure measurement may be limited by cavitation on the surface of the PVDF membrane. The rise times measured in the APL-UW and Anat-IU were shorter than in the other lithotripters (27 vs 55 ns). However, measured rise time is critically dependent on alignment of the hydrophone perpendicular to the shock wave axis. Misalignment by 5° produces an increase in rise time of 30 ns for a hydrophone with a 0.5 mm diameter active area (the peak pressure is reduced by only 2% for the same misalignment). The discrepancy in the rise time data was probably because it was easier to align the membrane hydrophone in the APL-UW and Anat-IU machines. Lastly the duration T_+ in the HM3-A lithotripter was shorter than in the other machines, probably because of the HM3 high-voltage circuitry has a slightly shorter time constant (Fig. 6). Given the expected shot-to-shot variation, the characteristics of the acoustic waveforms were very similar.

The dependence of peak positive and peak negative pressure on charging voltage is shown in Fig. 9. The values associated with each shot are marked by a cross ''+'' and the mean value by the solid line. Presenting the data in this manner provides information on the scatter of the data as well as the trends. In general, there was a monotonic increase in pressure with charging voltage with a tendency to saturate at the higher voltages, a phenomenon that has been reported previously with electrohydraulic lithotripters.[12] One exception was the nonmonotonic behavior of p_+ in the GALCIT lithotripter. We speculate that this is a statistical effect and is related to the limited number of shots we were able to measure at each condition. We show data below for another experiment with the GALCIT lithotripter that indicates monotonic behavior of p_+ with charging voltage.

The data for both the peak positive and peak negative pressures shown in Fig. 9 were separately subject to a two-way analysis of variance (ANOVA) to investigate pressure and machine differences and any interactions. All three terms were significant and some subanalyses were undertaken to define where the differences occur. Comparisons were made for voltage pooled across machines and for machines pooled across voltage using one way ANOVA with Tukey's HSD test for multiple comparisons. In addition, comparisons across machines within each voltage were made using one way ANOVA with Tukey's HSD test for multiple comparisons. Data for the peak positive pressure are shown in Table V. In general, the HM3-A and GALCIT lithotripters had slightly larger pressures (both $p+$ and $p-$) than the other three lithotripters (HM3-B, APL-UW, Anat-IU). The three Caltech lithotripters fall within the variation of the two HM3s. We note that the data are not identical in Tables IV and V. The data were obtained at identical conditions but during different experiments; Table V was from the voltage measurements (Fig. 9) and that in Table IV from the axial measurements (Fig. 10). The differences indicate the variability in the performance of an individual electrohydraulic lithotripter.

The axial distribution of the peak positive and negative pressures are shown in Fig. 10. In each case, the spatial maximum of the peak negative pressure occurred about 20

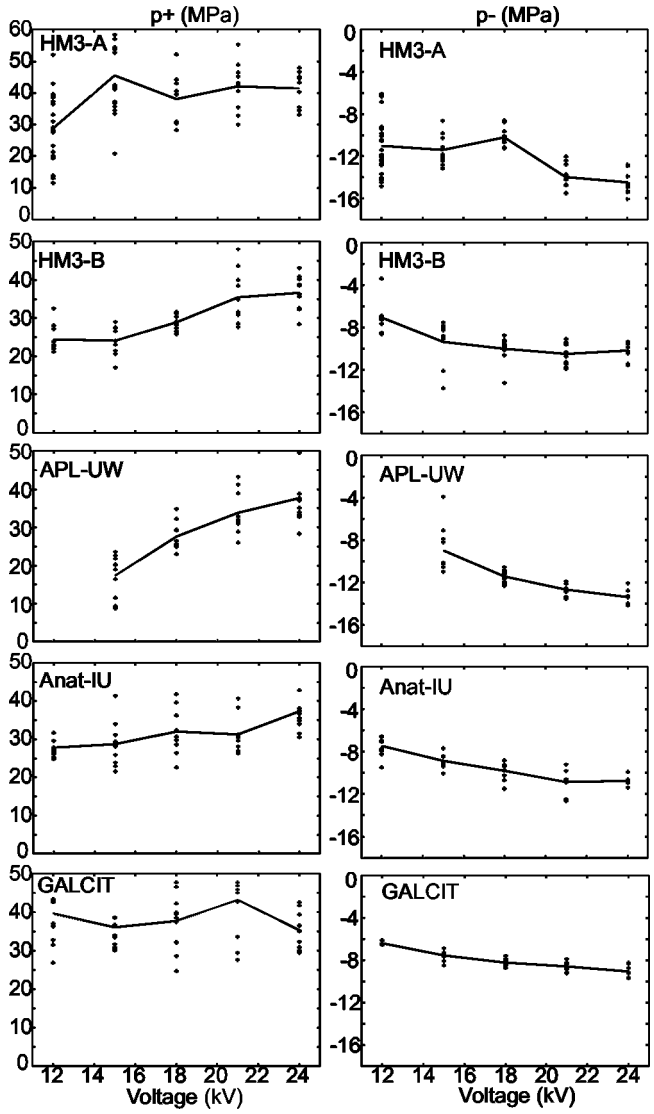

FIG. 9. Variation in $p+$ (left column) and $p-$ (right column) with charging voltage for the five lithotripters.

TABLE V. Comparison of peak-positive pressure for the five lithotripters as a function of charging voltage. Each entry is of the form: mean±standard deviation (number of measurements).

	12 kV	15 kV	18 kV	21 kV	24 kV
HM3-A	28.8±10.8(24)	45.5±11.6(17)	38.1±7.7(10)	42.1±7.7(10)	41.4±5.3(10)
HM3-B	24.4±3.7(10)	24.1±3.9(9)	28.9±2.0(10)	35.5±6.8(10)	36.7±4.5(10)
APL-UW	···	17.2±5.6(10)	27.6±3.7(10)	33.9±5.5(10)	37.7±7.1(10)
Anat-IU	27.8±2.4(10)	28.7±5.9(10)	32.0±5.9(10)	31.3±4.7(10)	37.3±6.2(10)
GALCIT	39.7±8.3(10)	36.1±8.0(10)	37.8±7.4(10)	43.2±10.3(10)	35.3±4.8(10)

mm in front of the location of the peak positive pressure. This was in agreement with other measured data[8] and with calculations of the HM3 pressure field.[24–26] In general, the peak positive pressure was 15 MPa at −50 mm and, depending on the machine, exceeded 20 MPa in the range −20 mm to −25 mm. The pressure peaked between 35 and 40 MPa around F2 and then decayed below 20 MPa somewhere between 30 and 50 mm. The 6 dB length of the axial field was approximately 60 mm for all five machines. This is also in agreement with other measurements and calculations. Note that the location of the maximum peak positive pressure may not be at the geometrical focus F2.

The lateral distribution of the peak positive and negative pressures are shown in Fig. 11. All the lithotripters had a 6 dB beamwidth of approximately 10 mm which was consistent with measurements and calculations reported elsewhere.[8,24,26] These results were for lateral scans perpendicular to the orientation of the electrode in the reflector. Scans parallel to the electrode orientation showed slight asymmetry due to shading by the electrode (data not shown).

C. Firing rate

We investigated the ability of the research machines to maintain consistent output over a range of clinically relevant firing rates. In clinical settings, the HM3 is typically syn-

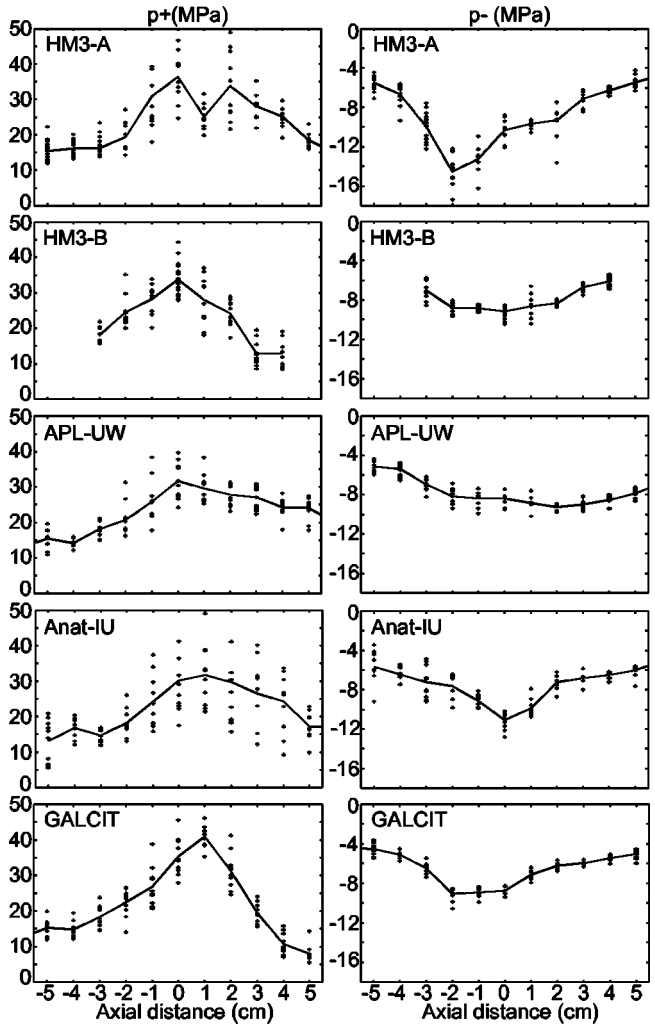

FIG. 10. Variation in $p+$ (left column) and $p-$ (right column) with axial location.

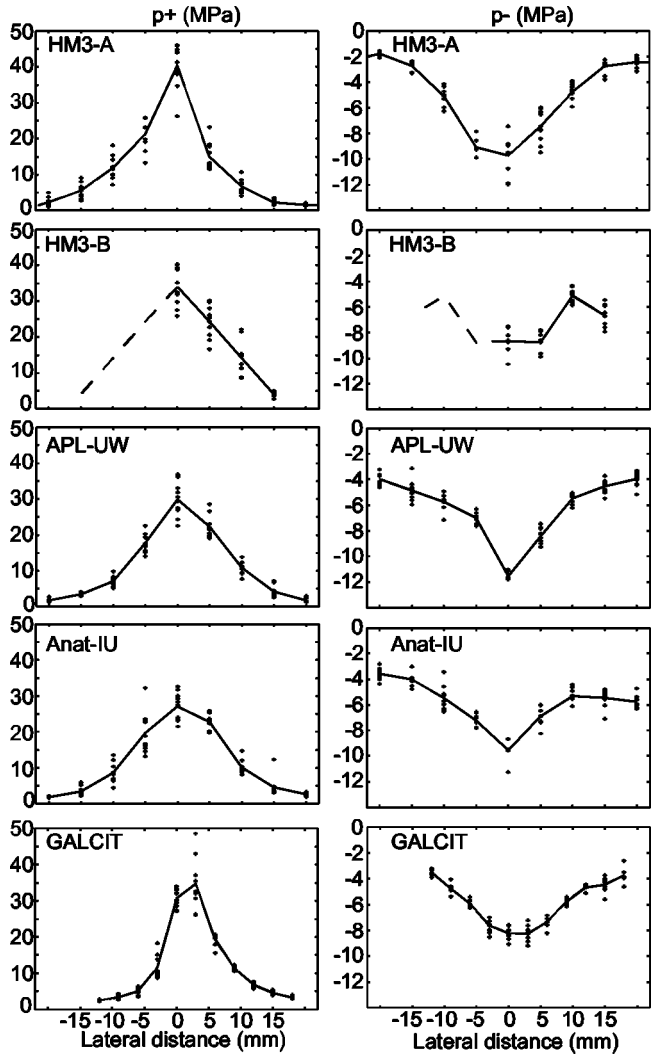

FIG. 11. Variation in $p+$ (left column) and $p-$ (right column) with lateral location.

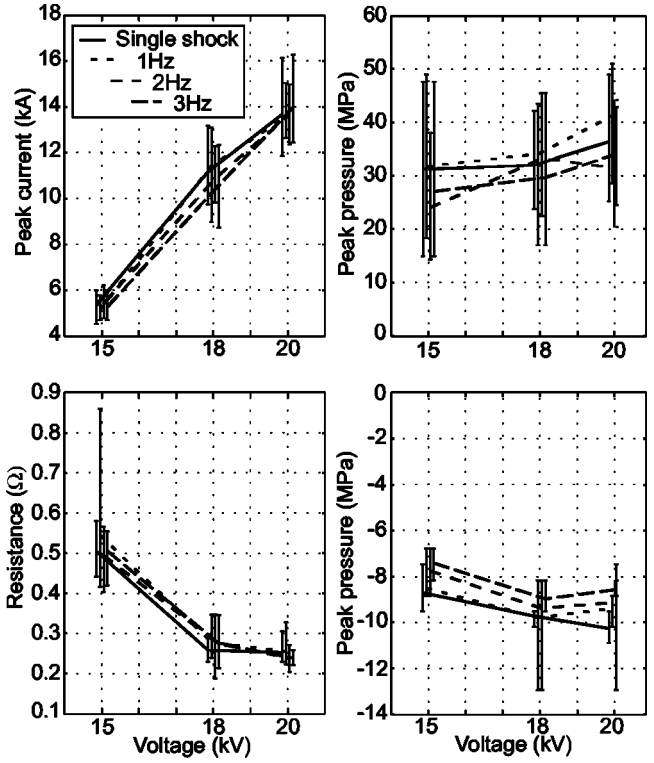

FIG. 12. Variation in critical parameters of the GALCIT lithotripter (resistance, inductance, peak positive pressure and peak negative pressure) as a function of firing rate and voltage.

chronized to the patient's heart beat and fired at 1–2 Hz. The synchronization is required because some patients suffer arrythmia if the discharge occurs in certain parts of the heart cycle, however, often it is possible to fire the HM3 faster. The clinical devices we used were capable of firing at rates up to 2.5 Hz using external triggering and even faster with the manual firing button. Figure 12 shows the variation in the the characteristics of the high-voltage system (discharge resistance and inductance) and the acoustical output (peak positive and peak negative pressures at the focus) as a function of voltage and firing rates in the GALCIT lithotripter. Note in this experiment, there was a monotonic increase in p_+ with voltage, cf. Fig. 9.

A two-way analysis of variance (ANOVA) of the data was carried out to determine the effect of voltage and firing rate on the output of the machine. The measured resistance and peak current were found to be independent of firing rate. They did, however, vary with voltage: the resistance was significantly higher at 15 kV and the peak current increased monotonically with voltage. The maximum peak positive pressure increased significantly with increasing voltage regardless of the pulse rate. The peak positive pressure did not vary significantly with pulse rate, except for a rate of 2 Hz which was statistically higher than a rate of 1 Hz. The magnitude of the peak negative pressure increased significantly with increasing voltage regardless of the pulse rate. The magnitude of the peak negative pressure decreased with increasing firing rate. This was the only parameter that varied with pulse rate and we suspect that it is due to cavitation induced bubbles collecting on the surface of the membrane hydrophone.

Finally, the pressures at the focus were measured over successive shots to ensure that the output remained constant. Figure 13 shows the peak pressures at the focus after 2, 10, and 20 shock waves at various firing rates. The voltage was held fixed at 18 kV. A one-way ANOVA indicated that neither peak positive pressure nor peak negative pressure were affected by the number of shots. These results indicate that the acoustic output of the Caltech lithotripters remains stable over consecutive shots, at various firing rates, and at various voltages.

IV. DISCUSSION

The Dornier HM3 is a commercial lithotripter. Its design and fabrication are proprietary and not accessible to scrutiny. Still, it was possible to take measurements that allowed us to

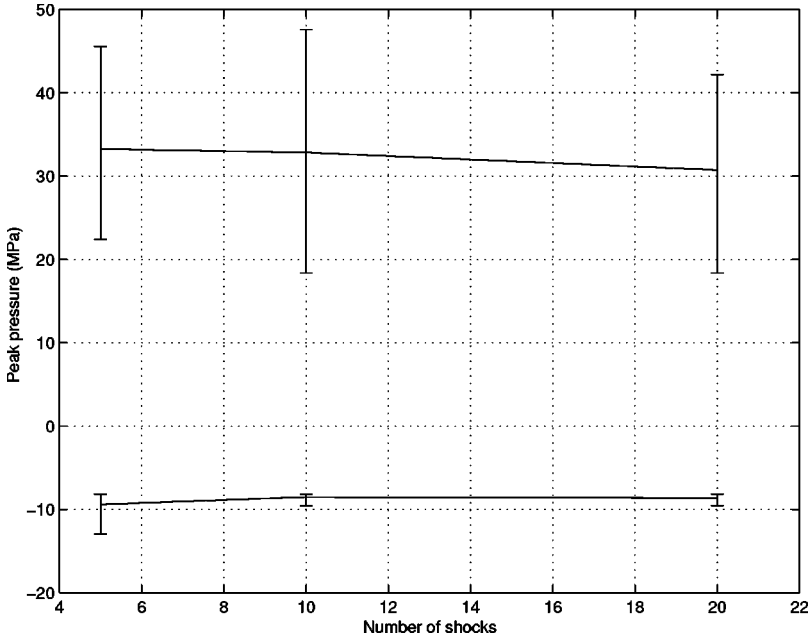

FIG. 13. Variation in peak positive pressure and peak negative pressure as a function of number of shots fired for various firing rates.

reproduce a number of mechanical and electrical features of this machine that are critical to its performance. Our strategy was to duplicate the geometry of the ellipsoidal reflector, use the same electrode, and attempt to reproduce the charging voltage, storage capacitance and impedance of the discharge circuitry.

Electrohydraulic lithotripters exhibit considerable shot-to-shot variability. This is a hallmark of the HM3 and may, indeed, contribute to its efficiency in breaking stones. We observed that measured fields in the research machines were not identical to those of the HM3; indeed the two HM3 lithotripters were not statistically equivalent. However, among the pulse parameters measured, only shock rise time differed substantially—a fact that can be attributed to difficulties in alignment within the HM3. For the peak positive and peak negative pressure, we found that the measurements among the three research machines were consistent, as the variation among them was no greater than the variation between the two HM3s. The equivalence of the acoustic fields means that other parameters which can be derived from the acoustic field, for example, pulse energy,[27] will also be consistent across the research and clinical machines. Thus, based upon our measurements of the shock wave field the research machines are equivalent to one another and appear to be equivalent to the HM3.

A further indication that the Caltech lithotripters are functionally equivalent to the HM3 comes from analyses of the cavitation fields generated by the two machines. We have observed that the APL-UW lithotripter generates cavitation bubbles that are comparable in number, size, and dynamics to those in the cavitation field of the HM3.[28] Given that the cavitation field is driven by the acoustic field this is further evidence of the similarity in the behavior of the machines.

There are minor weaknesses with the current design. For example, the water tank must be emptied in order to replace the electrode. Also, the tank does not have a recirculating degassing-filtering water system which means that during an experiment the water absorbs gas and dirt from the atmosphere making the water progressively more prone to cavitation.

The research lithotripters have already been used to investigate some aspects of lithotripsy. Experiments indicating a role for shear as a mechanism in tissue injury have been reported with the GALCIT lithotripter.[16] The APL-UW lithotripter has been fitted with a second power pack which allows two sparks to be fired within the tank. This configuration has been used to test an ellipsoidal reflector made from a pressure-release material.[19,29,30] Results indicate that the cavitation field at the focus of a pressure-release reflector is much less damaging than the cavitation field from a rigid (brass) reflector, even though the peak acoustic pressures are almost identical. These results have lead to the development of pressure-release inserts that can be used in a clinical HM3 for animal experiments.[31] The two spark system has also been used with two confocal rigid reflectors,[29] that is capable of both enhancing and mitigating cavitation. Cavitation has been controlled in the Anat-IU machine by means of overpressure.[32] The effect of air bubbles on *in vitro* cell systems has also been reported using the Anat-IU EHL.[33]

In conclusion, three research lithotripters have been built to mimic the behavior of the Dornier HM3 lithotripter. The critical electrical and mechanical parameters of the HM3 were matched in the design of the research machines. The three research machines were individually modified for specific applications, but their measured acoustic fields were equivalent to each other and equivalent to the acoustic fields measured in two clinical Dornier HM3 lithotripters. The performance of the research machines was shown to be stable for various firing rates and number of shock waves. The results indicate that experiments carried out in the research machines are directly relevant to the performance of a Dornier HM3.

ACKNOWLEDGMENTS

This work was funded by the National Institutes of Health through Grant No. DK43881. The authors thank Dr. George Keilman and Dr. O. A. Sapozhnikov for technical assistance and Dr. J. E. Lingeman and Dr. A. P. Evan for providing access to the HM3 lithotripters at Methodist Hospital.

[1] C. Chaussy, W. Brendel, and E. Schmiedt, Lancet **II**, 1265 (1980).
[2] J. E. Lingeman, in *New Developments in the Management of Uurolithiasis*, edited by J. E. Lingeman and G. M. Preminger (Igaku-Shoin, New York, NY, 1996), pp. 79–98.
[3] J. V. Kaude, C. M. Williams, M. R. Millner, K. N. Scott, and B. Finlayson, Am. J. Roentgenol. **145**, 305 (1985).
[4] A. P. Evan, L. R. Willis, B. A. Connors, J. A. McAteer, and J. E. Lingeman, J. Endourology **5**, 25 (1991).
[5] A. P. Evan and J. A. McAteer, in *Kidney Stones: Medical and Surgical Management*, edited by F. L. Coe, M. J. Favus, C. Y. C. Pak, H. J. Parks, and G. M. Preminger (Lippincott-Raven, Philadelphia, 1996), pp. 549–570.
[6] A. P. Evan, L. R. Willis, J. E. Lingeman, and J. A. McAteer, Nephron **78**, 1 (1998).
[7] B. Sturtevant, in *Smith's Textbook of Endourology*, edited by A. D. Smith, G. H. Badlani, R. V. Clayman, G. H. Jordan, L. R. Kavoussi, J. E. Lingeman, G. M. Preminger, and J. W. Segura (Quality Medical Publishing, St. Louis, MO, 1996), pp. 529–592.
[8] A. J. Coleman, J. E. Saunders, R. C. Preston, and D. R. Bacon, Ultrasound Med. Biol. **13**, 651 (1987).
[9] M. Müller, Biomedizinische Technik **34**, 62 (1989).
[10] M. Müller, Biomedizinische Technik **35**, 250 (1990).
[11] A. J. Coleman and J. E. Saunders, Ultrasound Med. Biol. **15**, 213 (1989).
[12] A. Buizza, T. Dell'Aqila, P. Giribona, and C. Spagno, Ultrasound Med. Biol. **21**, 259 (1995).
[13] A. J. Coleman, J. E. Saunders, and M. J. Choi, Phys. Med. Biol. **34**, 1733 (1989).
[14] S. R. Akers and F. H. Cocks, Inst. Tech. **23**, 50 (1989).
[15] F. E. Prieto, A. M. Loske, and F. L. Yarger, Rev. Sci. Instrum. **62**, 1849 (1991).
[16] D. Howard and B. Sturtevant, Ultrasound Med. Biol. **23**, 1107 (1997).
[17] D. G. Pellinen, M. S. Di Capua, E. Stephen, E. Sampayan, H. Gerbacht, and M. Wang, Rev. Sci. Instrum. **51**, 1535 (1980).
[18] A. R. Kaiser, C. A. Cain, E. Y. Hwang, J. B. Fowlkes, and R. J. Jeffers, J. Acoust. Soc. Am. **99**, 3857 (1996).
[19] M. R. Bailey, D. T. Blackstock, R. O. Cleveland, and L. A. Crum, J. Acoust. Soc. Am. **104**, 2517 (1998).
[20] R. A. Smith and D. R. Bacon, J. Acoust. Soc. Am. **87**, 2231 (1990).
[21] D. S. Campbell, H. G. Flynn, D. T. Blackstock, C. Linke, and E. L. Carstensen, J. Lithotripsy and Stone Disease **3**, 147 (1997).
[22] International Electrotechnical Committee, ''Ultrasonics - pressure pulse lithotripters - characteristics of fields,'' IEC standard 87/89A/CDV (1996).
[23] J. Staudenraus and W. Eisenmenger, Ultrasonics **31**, 267 (1993).
[24] M. A. Averkiou and R. O. Cleveland, J. Acoust. Soc. Am. **106**, 102 (1999).

[25] A. J. Coleman, M. J. Choi, and J. E. Saunders, Ultrasound Med. Biol. **17**, 245 (1991).
[26] P. T. Christopher, J. Acoust. Soc. Am. **96**, 3088 (1994).
[27] T. Dreyer, R. E. Riedlinger, and E. Steigar, in *Proceedings of the 16th International Congress on Acoustics*, edited by P. K. Kuhl and L. A. Crum (Seattle, WA, 1998), pp. 2811–2812.
[28] R. O. Cleveland, O. A. Sapozhnikov, and M. R. Bailey, J. Acoust. Soc. Am. **107**, 1745 (2000).
[29] M. R. Bailey, Technical Report ARL-TR-97-1, Applied Research Laboratories, The University of Texas at Austin, 1997.
[30] M. R. Bailey, D. T. Blackstock, R. O. Cleveland, and L. A. Crum, J. Acoust. Soc. Am. **106**, 1149 (1999).
[31] B. A. Connors, A. P. Evan, L. R. Willis, J. A. McAteer, J. E. Lingeman, R. O. Cleveland, M. R. Bailey, and L. A. Crum, J. Urol. (Baltimore) **159**, 32(A) (1998).
[32] M. A. Stonehill, J. C. Williams, Jr., M. R. Bailey, D. Lounsbery, R. O. Cleveland, L. A. Crum, A. P. Evan, and J. A. McAteer, Methods in Cell Science **19**, 303 (1998).
[33] J. C. Williams, Jr., M. A. Stonehill, K. Colmenares, A. P. Evan, S. P. Andreoli, R. O. Cleveland, M. R. Bailey, L. A. Crum, and J. A. McAteer, Ultrasound Med. Biol. **25**, 473 (1998).